Available online at www.sciencedirect.com
SCIENCE DIRECT®
ELSEVIER
Bioorganic & Medicinal Chemistry 12 (2004) 1835–1843
Bioorganic & Medicinal Chemistry

Specificity of neomycin analogues bound to the packaging region of human immunodeficiency virus type 1 RNA

Mark P. McPike, Jerry Goodisman and James C. Dabrowiak*

Department of Chemistry, Center for Science and Technology, R 1-014, Syracuse University, Syracuse, New York 13244-4100, USA

Received 6 August 2003; revised 28 January 2004; accepted 28 January 2004

Abstract—The packaging region of HIV-1 RNA contains a number of structural features which are important in the life cycle of the virus, making this segment of RNA a potential target for new types of AIDS-directed drugs. We studied the binding of three neomycin analogues (neo-guanidino, neo-acridine, and neo-neo) to a 171-mer RNA molecule from the packaging region of HIV-1 using quantitative footprinting and circular dichroism. Neo-guanidino produced footprinting patterns and effects on the CD similar to those observed for neomycin and paromomycin, indicating that all three compounds bind to the same regions of the 171-mer. Neo-guanidino binds to SL 1 where it joins the large internal loop, near a bulge in the stem of SL 1, and on SL 2. Neo-acridine, which has an acridine attached to neomycin, and neo-neo, which has two neomycins linked by a flexible tether, bind bivalently, and give very different footprinting and CD results from the other compounds. The neomycin portion of neo-acridine binds to the same sites as neomycin, while the attached acridine group appears to bind to a duplex region in the main stem of the folded 171-mer. Since the footprinting data for this analogue show few enhancements, bivalent binding of neo-acridine appears to stabilize the folded structure of RNA by effectively 'stapling' parts of the structure together. Neo-neo induces significant structural changes in RNA where neomycin binds. This may be related to the inability of both neomycins of neo-neo it find optimal binding sites adjacent to one another without changing RNA structure. The intensity of a strong negative CD band in the spectrum of ψ-RNA at 208 nm is sensitive to drug-induced changes in RNA structure. Neo-guanidino and neo-neo (also neomycin and paromomycin), which change RNA structure, cause an *increase* in intensity while neo-acridine, which induces little distortion to RNA, causes a *decrease* in intensity. Molecular modeling analysis shows that C-5′ of ribose of neo-acridine and neo-neo must be directed *away* from the binding pocket when these analogues are bivalently bound to RNA. This study showed how variations in the structure of aminoglycosides lead to different binding specificity to part of the packaging region of HIV-1. Such knowledge will be important in design of drugs to target this region.

1. Introduction

The activity of aminoglycoside drugs against Gram-negative bacteria is related to their ability to bind to the A-site of ribosomal RNA.[1,2] Since the drugs can also interact with eukaryotic RNA, the compounds exhibit toxic side effects that limit their extended use for treating bacterial infections.[3] In an effort to improve the antibacterial properties and broaden the pharmacological application of the aminoglycosides,[4] many recent studies have focused on how the drugs recognize RNA.

To explore the relationship between aminoglycoside structure and RNA binding affinity, Wong and co-workers[5] studied binding of neamine analogues to oncogenic mRNA sequences. They found that compounds having different substituents on the 5-position of neamine bind strongly to single-stranded breakpoints of Bcr-Abl and PAX3-FKHR mRNAs. Using thermal denaturation, fluorescence spectroscopy, and footprinting, Kirk and Tor[6] studied the binding of aminoglycosides to tRNA. They observed that kanamycin A, neomycin B and a synthetic dimer of the latter drug bind to the anticodon stem and the junction between the TψC and D loops of $tRNA^{phe}$.

Aminoglycosides can affect the function of RNA. Tobramycin, with an attached EDTA group, and neomycin joined to a second neomycin molecule, i.e., neo-neo, are more effective than their unmodified counterparts in inhibiting the catalytic function of the *Tetrahymena* ribozyme.[7,8] The effectiveness of neo-neo is related to its ability to bind in a bivalent manner to two adjacent

Keywords: Aminoglycosides; HIV-RNA; Footprinting; Circular dichroism.
* Corresponding author. Tel.: +31-5443-4601; fax: +31-5443-4070; e-mail: jcdabrow@syr.edu

0968-0896/$ - see front matter © 2004 Elsevier Ltd. All rights reserved.
doi:10.1016/j.bmc.2004.01.044

high-affinity sites on the ribozyme. Studies with the Rev response element (RRE),[9–13] and TAR RNA of human immunodeficiency virus HIV[14–17] showed that aminoglycosides can block proteins from binding to their interaction sequences. Thus, suitably modified aminoglycoside drugs could potentially control the spread of the virus that causes AIDS.

Despite numerous structural studies of aminoglycosides bound to RNA,[15,18–21] it is not yet clear which structural features of the drug and RNA control recognition. This is mainly due to the fact the drugs can easily change their shapes, allowing high-affinity interactions with a variety of different RNA sites. Earlier we reported[22–25] the results of footprinting, ultraviolet absorption, circular dichroism and UV melting studies on paromomycin and neomycin interacting with a large RNA molecule from the packaging region (ψ-element) of HIV-1 (LAI). The RNA molecule, a 171-mer, is shown in Figure 1. It contains the initiation site for the formation of the HIV-RNA dimer (DIS) and it is an important binding region for the nucleocapsid protein, NCp7.[26] In this report we use quantitative footprinting, CD and molecular modeling to study the binding of three neomycin analogues: neo-neo, neo-acridine, and neo-guanidino (Fig. 1) to the packaging region of HIV-1 (LAI).

2. Results

2.1. Footprinting

The footprinting gels for neo-neo, neo-acridine, and neo-guanidino are shown in Figures 2–4 and selected footprinting plots for these compounds in the region 230–255 are shown in Figure 5. Initial slopes of footprinting plots for the three neomycin analogues as well as for neomycin itself and paromomycin are shown in Figure 6 along with the standard errors in the slopes. For negative slopes, it is the relative initial slope (initial slope divided by zero-drug intercept) that is shown, as this should be proportional to the binding constant of the analogue toward RNA.

For neo-guanidino, footprinting data for higher-numbered positions could not be obtained. At higher drug concentrations, single nucleotide resolution is lost at site locations greater than ~310 and oligomers with apparent lengths greater than that of the full length 171-mer appear at the top of the autoradiogram (data not shown). The reason for this is not clear, but it may be that neo-guanidino facilitates interstrand RNA-RNA associations for the longer RNA oligomers which persist under denaturing conditions in the gel. Attempts to eliminate the associations by using formamide loading buffers and/or heating footprinting samples prior to

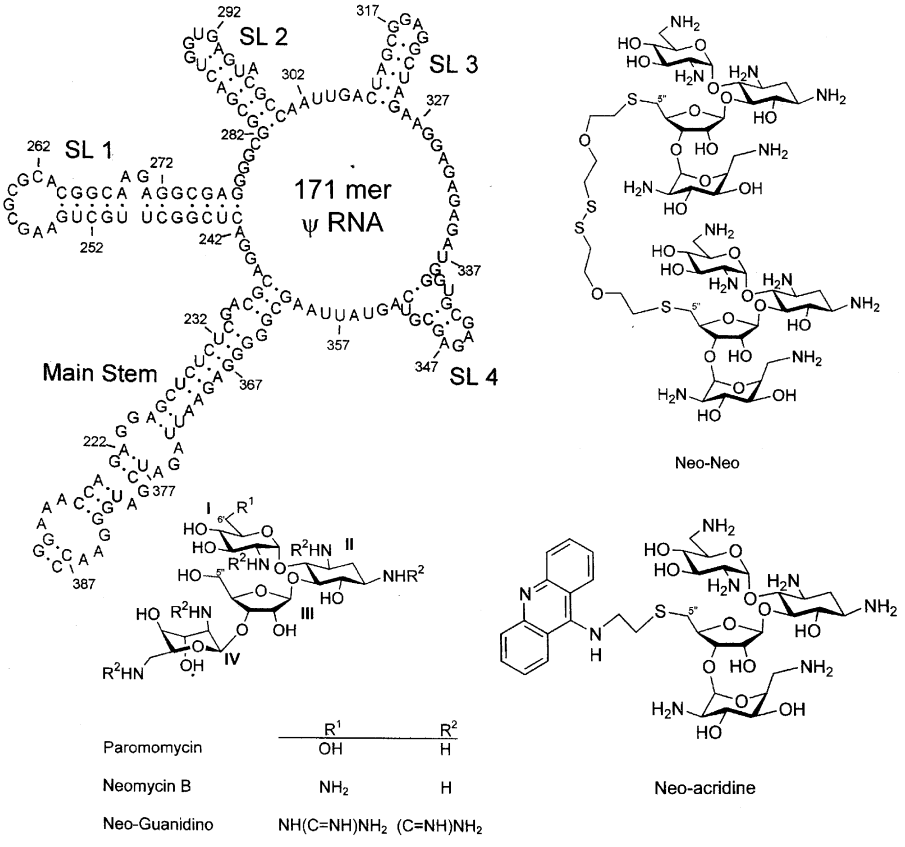

Figure 1. Structures of the 171-mer ψ-RNA from the packaging region of HIV-1 (LAI) and aminoglycoside analogues used in the study.

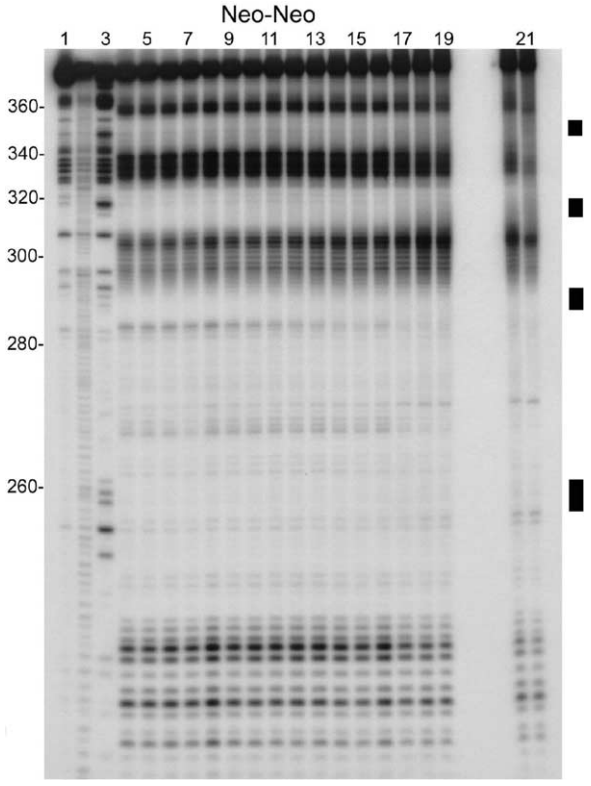

Figure 2. Footprinting autoradiogram (9% polyacrylamide gel) of neo-neo and ψ-RNA (1.1 μM) using RNase I as a cleavage agent. Lane 1 contains RNA alone; lane 2, base (OH^-) hydrolysis ladder; lane 3, G ladder generated using 17 units of RNase T1. Other lanes correspond to drug concentrations (μM) as follows: 4, 0; 5, 0.5; 6, 0.75; 7, 1; 8, 2; 9, 3; 10, 4; 11, 5; 12, 6; 13, 7; 14, 8; 15, 9; 16, 10; 17, 11; 18, 12; 19, 13; 20, 14; 21, 15. The black bars on the right identify the approximate locations of SL 1 (bottom), SL 2, SL 3, and SL 4 (top).

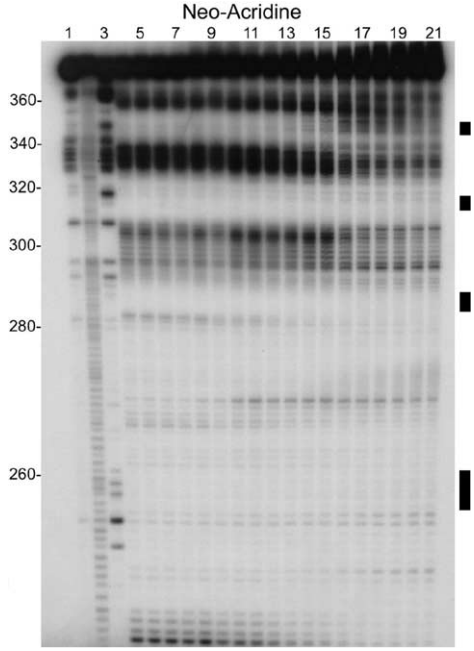

Figure 3. Footprinting autoradiogram (9% polyacrylamide gel) of neo-acridine and ψ-RNA (1.1 μM) using RNase I as a cleavage agent. See the caption for Figure 2 for lane identification, drug concentrations, and annotations.

loading into the gel had little effect. The loss of resolution limited the useful footprinting data for this analogue to sites below about 310, see Figure 6c.

The binding regions are shown by the negative slopes in Figure 6. In almost every case, the magnitude of the (relative) slope is small at the ends of a binding region and increases monotonically to a maximum at the middle. Possible interpretations of this pattern are (a) the drug binding site is in the center of the region so bound drug blocks cleavage at sites near the ends of the region less well than sites near the middle or (b) the region contains two or more drug sites having similar binding affinities. In the latter case cleavage sites near the middle of the region can be blocked by drug binding at more than one site but, at the ends of the binding site, only one binding event inhibits cleavage.

The regions of positive slopes show the same pattern: small magnitude of the slope at the ends, increasing to a maximum at the middle. The positive slopes indicate drug-enhanced cleavage, which we believe arises from structural distortions caused by drug binding at sites outside the region showing enhancement. Cutting at a modified region, i.e., single-stranded RNA, would be expected to be larger in the middle of the region than the ends, where the region joins more ordered structure. The enzyme RNase I cleaves mainly in single-stranded regions of RNA.

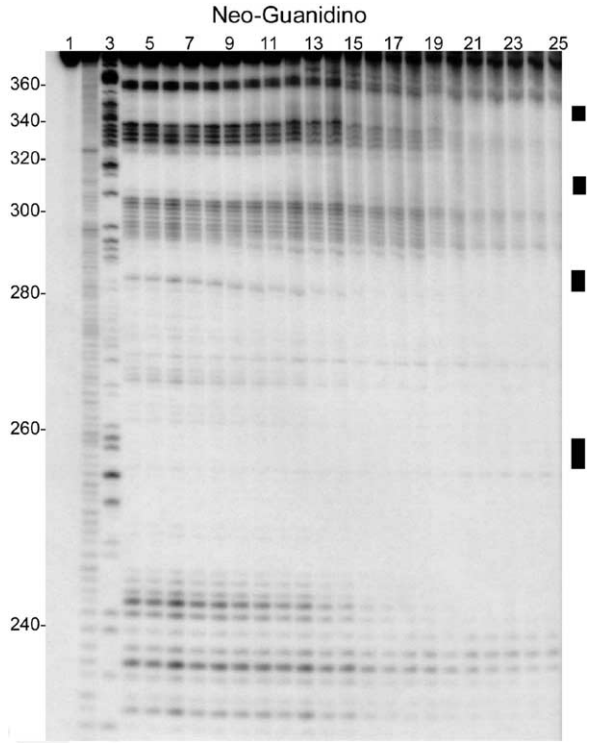

Figure 4. Footprinting autoradiogram (9% polyacrylamide gel) of neo-guanidino and ψ-RNA (1.1 μM) using RNase I as a cleavage agent. Lane 1 contains RNA alone; lane 2, base (OH^-) hydrolysis ladder; lane 3, G ladder generated using 17 units of RNase T1. Other lanes correspond to neo-guanidino concentrations (μM) as follows: 4, 0; 5, 0.2; 6, 0.5; 7, 1; 8, 2; 9, 3; 10, 4; 11, 5; 12, 6; 13, 7; 14, 8; 15, 9; 16, 10; 17, 11; 18, 12; 19, 13; 20, 14; 21, 15; 22, 16; 23, 18; 24, 20; 25, 25. The black bars on the right identify the approximate locations of SL 1 (bottom), SL 2, SL 3, and SL 4 (top).

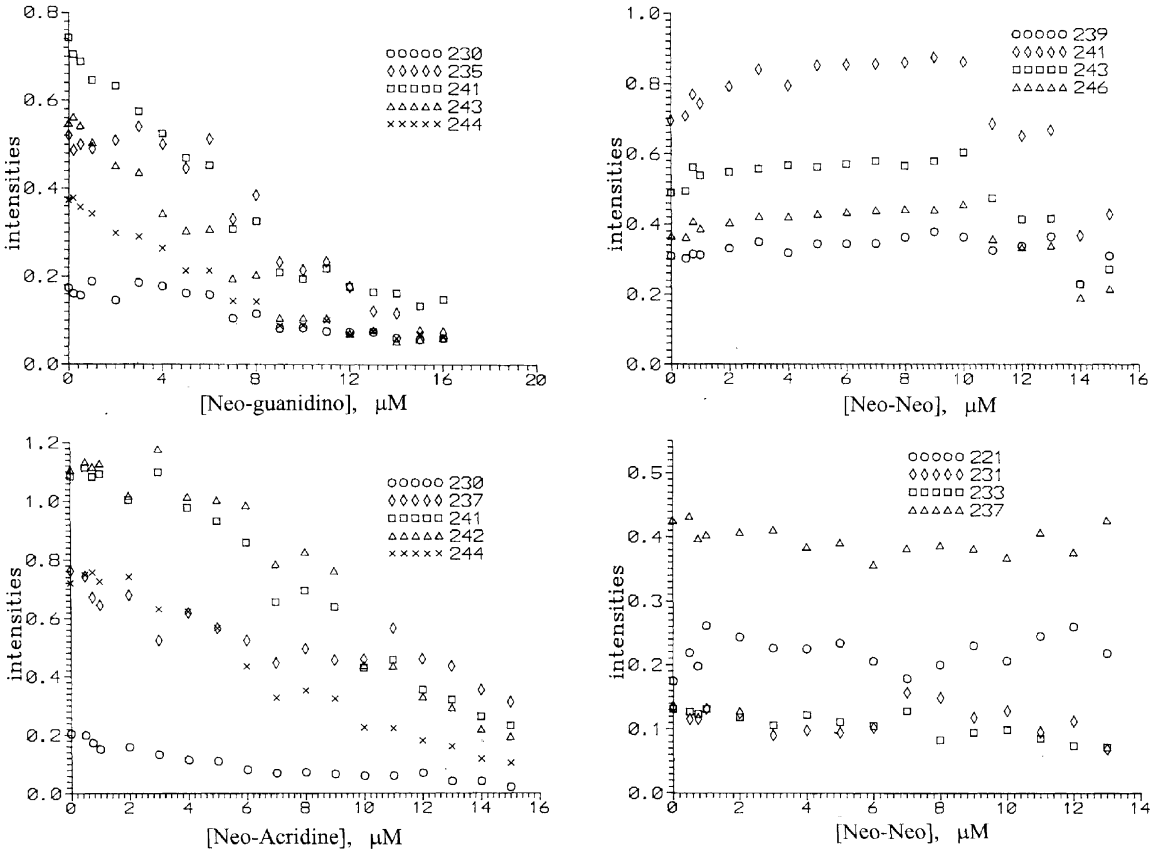

Figure 5. Representative footprinting plots for neo-guanidino, neo-acridine, and neo-neo for sites in the region 230–246 of the RNA. The plots for neo-guanidino and neo-acridine are all type 1, showing drug binding; the plots for neo-neo are type 1 and type 2, the latter showing enhanced cleavage due to changes in RNA structure.

2.1.1. Neomycin, paromomycin, and neo-guanidino. Inspection of the slope plots in Figure 6 shows that neomycin, paromomycin, and neo-guanidino behave similarly in the region 230–300, exhibiting three broad binding regions near sites 243, 268, and 282 on ψ-RNA. On the proposed secondary structure shown in Figure 1, these regions are located where SL 1 joins the large internal loop, near a small bulge in the stem of SL 1, and where SL 2 joins the internal loop. As noted, the initial relative slope should be proportional to the binding constant K, making it a measure of the affinity of the drug for the site. Although the errors (Fig. 6) are larger for paromomycin than for the other drugs, the values of K for the drug sites near 243 and 268 appear similar for all three compounds.

In contrast, neomycin seems to have a lower affinity than the other two drugs for the third drug site, near 282. However, the neomycin footprinting plots in this region are unusual, as discussed previously.[24] Intensities do not decrease monotonically with drug concentration, as for typical binding-site plots. As a result, initial relative slopes, calculated from a linear fit of the first 12–14 points, do not have the same significance for sites in this region as for the others.

Both neomycin and neo-guanidino cause a structural change near site 232, which is near the bulge in the main stem, Figure 1. Paromomycin does not seem to show the same effect. All three drugs show a region of structural change centered at about 300. For neo-guanidino, the lack of data for sites numbered above 310, mentioned previously, makes it impossible to tell where this region ends. For the other two drugs, it seems to extend from about 295 to 305.

For locations numbered above 300, neomycin and paromomycin show clear differences. The former exhibits binding at ~332, in the homopurine tract in the large internal loop, Figure 1, but no structural changes (although there are not many usable footprinting plots for nearby regions). The latter causes structural changes, but no binding, between 315 and 370. These occur in the regions: around location 330, where SL 2 joins the internal loop, and around location 355, in the internal loop.

2.1.2. Neo-acridine. This analogue exhibits six or seven drug binding regions, of which four are well-defined. These four are centered at ~230 (in the main stem), ~242 (where SL 2 joins the internal loop), ~285 (in SL 2), and ~335 (in the homopurine tract). There may also be binding sites at ~312 (where SL 3 joins the internal loop), but errors in slopes are large here, and at ~360 (where the main stem joins the internal loop), defined by only two points. There is also a weak site centered at

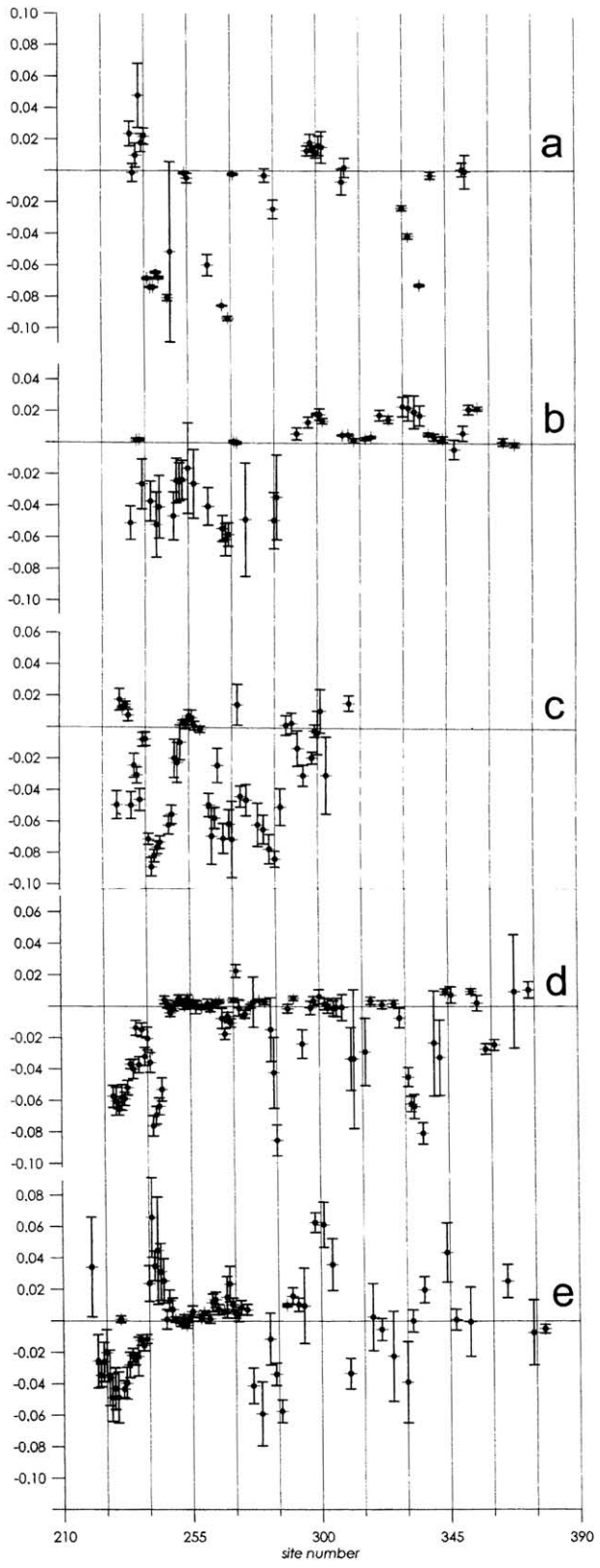

Figure 6. Slopes from linear fits of the low-drug portions of the RNase I footprinting plots (see text) with error bars. The plots are for neomycin (a), paromomycin (b), neo-guanidino (c), neo-acridine (d), and neo-neo (e). The site number refers to the numbering system for HIV-1 (LAI) of the 171-mer RNA, Figure 1. Negative slopes indicate binding and positive slopes identify sites of drug-induced structural change. The negative slopes have been divided by the *y*-intercepts to give relative slopes, whose magnitude should be proportional to binding affinity.

~269, in the bulge of SL 1. Binding near 295 is questionable because it is shown by only one footprinting plot. When compared to the other binding locations, the sites at ~285 and ~312 are relatively narrow, 4–5 nt long, Figure 6d.

Neo-acridine induces very few structural changes (enhancements) in ψ-RNA, and these are weak, as evidenced by the small magnitude of the positive slopes. The enhancement shown for site 271 is questionable because it involves only a single site, rather than a group of contiguous sites as for the other compounds.

2.1.3. Neo-neo. This analogue exhibits binding sites that are broader (~18 nt long) than those for the other compounds. The sites are located near 228, in the main stem; near 280, between SL 1 and SL 2; and near 320, in SL 3 and the adjoining homopurine tract. Errors in the slopes are large for this compound, so there is a lot of

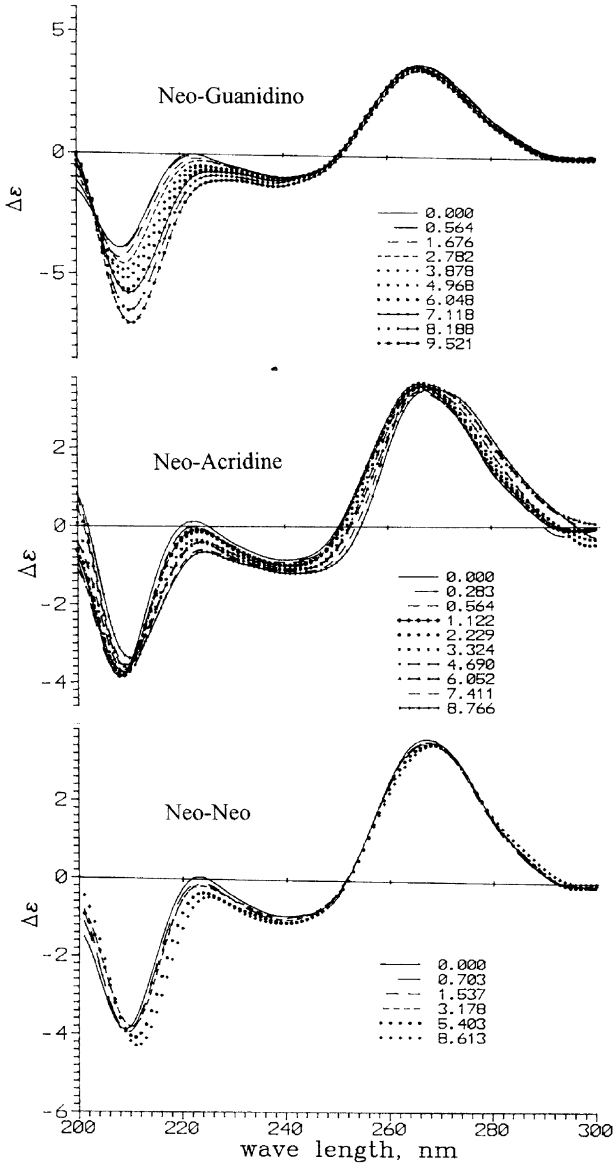

Figure 7. Circular dichroism spectra of ψ-RNA (0.5 μM) in the presence of various concentrations of analogue (stated on the plots). The quantity Δε has units of M^{-1} cm^{-1} nucleotide^{-1}.

uncertainty relative to the latter two regions. Interestingly, each binding region is followed in sequence by a region of structural change. These regions of structural change are centered near 242, where SL 1 joins the internal loop; near 300, where SL 2 joins the internal loop; and near 345, in SL 4.

2.2. Circular dichroism

As is shown in Figure 7, the 171-mer has CD bands at 266, 240 and 208 nm, with values of $\Delta\varepsilon$ (M^{-1} cm^{-1} $nucleotide^{-1}$) of +3.9, −0.8, and −3.6, respectively. The drugs themselves absorb much less than does the RNA in this region of the spectrum. The CD spectrum indicates that the RNA has considerable A-form secondary structure.[27] Figure 7a shows some of the CD plots for the 171-mer in the presence of neo-guanidino. In the range 0–10 μM, CD intensities for the wave length region, 205–225 nm, become markedly more negative with increasing drug concentration, and there is an isoelliptic point at 204 nm. However, little change is observed elsewhere in the spectrum. This behavior, including the location of the isoelliptic point, is very similar to that of neomycin[24] and paromomycin.[23]

In Figure 7b are shown CD intensities of ψ-RNA in the presence of various concentrations of neo-acridine. Although the changes in CD intensities with drug concentration are relatively small for this drug as compared to neomycin, paromomycin and neo-guanidino, they occur at all wave lengths between 200 and 300 nm. The negative peak in $\Delta\varepsilon$ at 208 nm becomes *less negative* as drug concentration increases. whereas $\Delta\varepsilon$ becomes more negative at higher wave lengths. The decrease in the magnitude of the negative CD band at 208 nm for neo-acridine contrasts with what is observed for the other analogues, for which increased drug concentration *increases* the intensity of this band. For frequencies up to 270 nm, the value of $\Delta\varepsilon$ is higher (more positive or less negative) for higher neo-acridine concentrations, but then the pattern reverses again. Thus, there appear to be isoelliptic points at 270 nm and 212 nm. As with the other analogues,[24] very high concentrations of drug cause large changes in CD intensity at all wavelengths (not shown), probably not related to structural changes induced by drug binding.

Some of the CD spectra of the 171-mer in the presence of neo-neo are shown in Figure 7c. Increasing the concentration of neo-neo up to 8.6 μM causes the CD intensity in the region 200–230 nm to become gradually more negative (increase in intensity), but produces little or no change in intensity at other wavelengths. There seem to be isoelliptic points at ~210 and ~252 nm. This behavior is similar to that earlier observed for neomycin, paromomycin and neo-guanidino, but the changes in the 200–230 nm region are less than those produced by the monomeric compounds. At high drug concentrations the magnitude of the CD intensity falls off rapidly at all wave lengths, probably indicating that neo-neo is causing precipitation of the RNA.

3. Discussion

The slope plots obtained from the footprinting data, Figure 6, show that neomycin, paromomycin and neo-guanidino bind to ψ-RNA in a similar manner. All three compounds bind near 242, where SL 1 joins the large internal loop of the RNA, near a small bulge in SL 1, ~267, and in the stem of SL 2. Neomycin and neo-guanidino also produce a structural change at ~235, near a bulge in the main stem. Structurally, neomycin and paromomycin differ only in the group on C-6′ of ring I (see Fig. 1) but, as was earlier discussed,[24] this structural difference leads to differences in the footprinting behavior of certain sites for the two compounds. Compared to neomycin and paromomycin, neo-guanidino is larger and has different hydrogen-bonding properties. The increased size of this analogue may be the reason why many sites in SL 2, including the loop, appear to bind drug, Figure 6c.

The changes in the CD spectrum of ψ-RNA induced by neomycin, paromomycin, and neo-guanidino are similar[23,24] (Fig. 7). All three analogues cause the

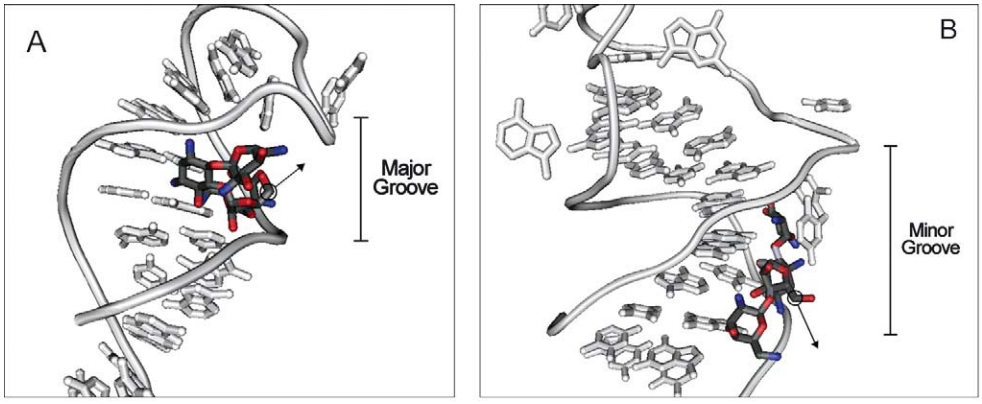

Figure 8. Molecular modeling analysis of neomycin bound to (A) the tau exon 10 splicing regulatory element, PDBID: 1EI2,[20] and (B) Tar hairpin of HIV-1 RNA, PDBID: 1QD3.[15] Shown is the orientation of neomycin (black) bound in the respective groove of each RNA hairpin (gray). The white circle indicates the location of the C-5′ of ribose (ring III), the site of attachment of the tether in neo-acridine and neo-neo. An arrow is drawn along the C-4′/C-5′ bond axis to indicate the approximate direction of the tether into solvent.

strong negative CD band of the 171-mer to intensify and shift slightly to lower energy. These changes are characterized by an isoelliptic point at 204 nm.

As previously noted, drug-induced changes in the absorption[25] and CD spectra[23] of the 171-mer occur for lower drug concentrations than does decreased cleavage observed in footprinting plots. This 'delayed binding' effect in footprinting could be due to competition between the drug and the enzyme for specific RNA sites, which would cause footprinting to report binding constants that are smaller than their true values.

As is evident from Figures 5–7, footprinting and CD data for neo-acridine and neo-neo are very different from those for the simpler analogues. This appears to be due to the fact that these analogues can bind to RNA in a bivalent manner. Analysis of structures of aminoglycoside-RNA complexes,[15,19–21] using molecular modeling programs, revealed that paromomycin and neomycin can adopt several conformations within the RNA binding pocket. Most of the structures show rings I and II, the neamine core, in direct contact with RNA, underscoring the importance of these rings in determining binding specificity. As is shown in Figure 1, both neo-acridine and neo-neo have a substituent attached to C-5′ of ring III, the ribose ring. If the neamine core of these analogues is involved in recognition and is in direct contact with RNA, C-5′ of ring III must be *directed into solvent*, away from RNA. With this orientation the group at the end of the tether can bind to another site on RNA, producing bivalent binding. Precedent for C-5′ pointed away from RNA can be found in the structures of neomycin bound to the RNA hairpins HIV-1 TAR[15] and tau exon 10 splicing regulatory element,[20] shown in Figure 8. Figure 8a shows tau exon splicing element, with the drug in the major groove spanning ~4 nt near the base of a 6 nt loop. Ring IV, buried in the major groove, is involved in intramolecular hydrogen bonding with sites on ring II, causing C-5′ of ribose (white circle) to be directed toward solvent, as indicated by the arrow. A similar orientation of C-5′ of ribose directed into solvent is found for HIV-1 TAR, Figure 8b. In this case the drug is in the *minor* groove and the neamine core is covered by a uridine-rich bulge. Since footprinting data show that neo-acridine and neo-neo bind in SL 1 similarly to neomycin and paromomycin, we suggest that the neo-acridine and neo-neo bind bivalently, with the neomycin domain bound to SL 1 and the tethered group bound to another RNA site spatially close to SL 1.

That neo-neo and neo-acridine bind to ψ-RNA in a bivalent manner is supported by the footprinting slope plots in Figure 6, which show they exhibit different binding/structural effects from the simpler analogues. The differences in binding between neo-acridine and neo-neo can be explained by considering the binding mechanisms used by the groups attached to the tether, acridine in the case of neo-acridine and neomycin in the case of neo-neo. Figure 6d shows that neo-acridine binds without distorting RNA, i.e., very few footprinting plots have positive initial slopes. Since an intercalation site for acridine is likely to be 'within reach' when the neomycin portion of the compound is bound to its high-affinity site, neo-acridine could bind bivalently without significantly altering RNA conformation. In fact, bivalent binding could have the effect of 'stapling' the structure together, making it less prone to conformational changes in successive binding events. Figure 6 also shows that the neomycin part of neo-acridine is bound to the same regions (SL1) used by neomycin, paromomycin and neo-guanidino, suggesting that the binding in the duplex region of the main stem (near 230) is due to the tethered acridine.

The neo-neo analogue has tethered neomycin moieties, each of which has high binding specificity toward ψ-RNA. Binding of one neomycin to a high-affinity site would either force the second neomycin to accept a site within the tether distance of the first site or induce a structural change in RNA to provide a second high-affinity site for the second neomycin. As is evident from the slope plots in Figure 6e, neo-neo is the most effective compound for inducing structural changes in RNA, implying that neomycin's high susceptibility leads to the second result. While all other analogues show binding between the main stem and SL 1 (~242), and near the bulge in SL 1 (~268), neo-neo induces structural changes at these locations. The number of drug molecules bound to ψ-RNA is not known, but a single neo-neo molecule might bind both to the main stem (~229) and where SL 1 joins the internal loop (~277), and bringing these regions into proximity requires structural changes near 242 and 268. Additional work with other analogues may determine if this is the case.

As shown in Figure 7, all of the analogues, including neomycin[24] and paromomycin,[24] shift the negative CD band at ~208 nm to lower energy. The shift in the position of this band is accompanied by an *increase* in its intensity, except for neo-acridine, for which the intensity of the band *decreases*. Since neo-acridine causes little structural change in the RNA molecule, an *increase* in the intensity of the CD band at 208 nm may be associated with ligand-induced structural change in RNA. Additional studies examining this phenomenon are warranted.

4. Conclusions

In this work we use quantitative footprinting, CD, and molecular modeling to study the binding of three neomycin analogues to a 171-mer RNA from the packaging region of HIV-1 (LAI). One of the analogues, neo-guanidino, which has the amino groups of neomycin changed to guanidinium moieties, binds in a region of the 171-mer where SL 1 joins the large internal loop, near a bulge in the stem of SL 1, and at numerous sites in SL 2. Both the footprinting data for this analogue and the effects that it has on the CD spectrum of the 171-mer are similar to those observed for neomycin and paromomycin. The results for neo-acridine and neo-neo are different, suggesting bivalent binding to RNA. Analysis using molecular modeling indicates that bivalent binding requires that C-5″ of ribose, the site of attachment of

the tether, be directed away from the binding pocket and into solvent.

The neomycin portion of neo-acridine interacts with sites observed for neomycin itself, while the acridine group appears to bind in a duplex region in the main stem. Among the compounds studied, neo-acridine is unique in that it binds without significantly distorting RNA structure. The neo-neo analogue binds to some sites used by neomycin, but it also induces significant structural changes. These occur where neomycin itself shows binding, where SL 1 joins the large internal loop, and near a bulge in SL 1. Since this analogue consists of two 'structure-reading' elements separated by a flexible tether, optimal binding of both elements requires RNA to alter its conformation.

In addition to footprinting, the change in intensity of the strong negative CD transition at 208 nm of the ψ-RNA can be used to detect structural changes induced by the compounds. This study demonstrates the power of combining quantitative footprinting methods with CD and molecular modeling for analyzing ligand binding to complex RNA structures.

The packaging region of the HIV genome is important for viral function. It facilitates the formation of the RNA dimer, helps in efficient packaging of the genome into the viral particle, and participates in reverse transcription during infectivity.[26] In view of the importance of this segment of RNA in the life cycle of the virus, it makes sense to target the region with small molecules that can disrupt its function.[28] However, the small molecule or drug must be able to identify HIV RNA, and specifically this region of the genome, in the presence of many competing RNA structures that are normally present in the biological milieu. The ability of aminoglycosides to target the A-site of ribosomal RNA[29,30] offers encouragement that this strategy will work. Success along these lines requires collecting more information on how drug and RNA structure influence where a ligand binds to RNA, i.e., its specificity.[31] The results of this study should be helpful to those interested in improving the RNA binding specificity of the aminoglycosides so that they realize their potential as new class of AIDS-directed drugs.

5. Experimental

5.1. Footprinting

The RNA was synthesized using T7 RNA polymerase in the presence of a DNA template, gel purified and 5′ end-labeled with ^{32}P according to published procedures.[22–24] The 171-mer RNA is missing the pentamer 5′-AAAUU at positions 303–307 of HIV-1 (LAI). The indexing system shown in Figure 1 has been adjusted to reflect this deletion.

The footprinting experiments were similar to those described earlier for neomycin[24] and paromomycin.[22,23] To summarize, the reactions were carried out in 10 μL of the buffer (10 mM Tris–HCl, pH 7), containing ~1.15 μM RNA, (~5% radiolabeled) using the enzyme RNase I (Ambion). The final drug concentrations used in the experiments are given in the captions to Figures 2 and 4. The footprinting solutions were prepared by adding various amounts of drug to the reaction mixture (drug concentrations were determined by weighing), waiting 30 min, and adding the enzyme in a volume of 1 μL. The time period for cutting was determined by analysis of cleavage fragments using a 9% denaturing PAGE gel. Reaction conditions which resulted in ~30% cleavage ('single hit kinetics') were: 0.04 U RNase I, 1.5 min, ~21 °C.

The footprinting reactions were terminated by the addition of 5 μL of the gel loading buffer containing 8 M urea (National Diagnostics) and 1mg/mL bromophenol blue. Eleven microliters of each footprinting reaction was loaded into denaturing 9% polyacrylamide gels and products were separated by electrophoresis. A number of footprinting experiments with electrophoresis for different lengths of time, or in different percentage gels, were carried out (data not shown). Autoradiographic films having band intensities in the linear response range of the film (see Figures 2–4) were scanned, images analyzed with SigmaScan, and band intensities determined. After correction for cutting and loading errors for each lane (<15%), intensities in control lanes were subtracted. Intensities for sites for which fragments are observed in the control lane are less accurate because of this subtraction. Sequence was determined by measuring locations on the gel for bands from the RNase T1 cleavage ladder. From plots of sequence versus location of these bands on the gel one could calculate the site number for any band from its location.

Representative footprinting plots, showing how band intensity changes with drug concentration, are shown in Figure 5 for sites in the region 230–246. In order to determine the locations of drug binding and regions of structural change, the initial slopes of the plots were calculated by fitting the low-drug portions of footprinting plots to lines. Only footprinting plots showing optical densities above 0.04 were used. Plots of slopes vs. site number for neo-guanidino, neo-neo, and neo-acridine as well as for neomycin[24] and paromomycin[22,23] are shown in Figure 6.

It was expected that many footprinting plots would be type 2,[22,23] with intensities increasing with drug concentration to a maximum, and decreasing thereafter. In order to consider only monotonic parts of the footprinting plots, we used 6–8 concentration points for the linear fits. When a positive slope was obtained, indicating enhanced cleavage due to a drug-induced structural change, the slope and its standard error were plotted (Fig. 6). When the slope was negative, indicating inhibition of cleavage due to drug binding (type 1 plot), we recalculated slopes using 12–14 concentration points and divided the calculated slope by the calculated intercept to obtain a relative initial slope, which was plotted, with its standard error, in Figure 6. Relative slopes were used when slopes were negative because they should be proportional to drug binding constants.[23]

5.2. Circular dichroism

Circular dichroism titrations were carried out at 21 °C using an Aviv model 202 CD instrument as earlier described.[23,24] The starting volume was 350 μL with the concentration of RNA being 0.5 μM in the buffer, 10 mM Tris–HCl (pH 7.0). After correcting for dilution due to the addition of the solution containing the drug (<10%), the CD spectra were smoothed using FFT filtering (PeakFit). The resulting circular dichroism spectra of ψ-RNA in the presence of various amounts of the analogues are shown in Figure 7. The drugs studied do not absorb at the wave lengths used (200–300 nm) for these studies, except for neo-acridine, which absorbs much less than does the RNA. Thus, the effects observed are due to conformational changes in the RNA oligomer.

5.3. Molecular modeling

The structures of neomycin and paromomycin bound to RNA, obtained from X-ray structural data[18] or solution NMR analyses,[15,19–21] were analyzed using the program CnD3, v. 4.0, available through the National Center for Biotechnology Information, Bethesda, MD. This program allows rotation, rendering, and annotation of structures available through the Protein Data Bank, PDB. Additional molecular modeling of structures in the PDB was carried out using HyperChem (Hypercube, Inc.) v. 5.1 and Insight II (Tripos, Inc.).

Acknowledgements

The research was supported in part by the NIH (GM32691 to P. N. Borer) and in part by the Chemistry Department, Syracuse University. We are very grateful to Professor Y. Tor (U. of California, San Diego) for samples of neo-guanidino, neo-acridine, and neo-neo and for helpful discussions pertaining to the work.

References and notes

1. Cundliffe, E. *Rev. Microbiol. Annu.* **1989**, *43*, 207.
2. Moazed, D.; Noller, H. F. *Nature* **1987**, *327*, 389.
3. Chambers, H. F.; Sande, M. A. In *Goodmans & Gilman's The Pharmacological Basis of Therapeutics*, 9th ed., Hardman, J. G.; Limbird, L. E.; Molinoff, P. B.; Ruddon, R. W.; Gilman, A. G. (Eds.). McGraw-Hill, NY, 1103.
4. Werstuck, G.; Green, M. R. *Science* **1998**, *282*, 296.
5. Sucheck, S. J.; Greenberg, W. A.; Tolbert, T. J.; Wong, C.-H. *Angew. Chem. Int. Ed.* **2000**, *39*, 1080.
6. Kirk, S. R.; Tor, Y. *Bioorg. Med. Chem.* **1999**, *7*, 1979.
7. Wang, H.; Tor, Y. *Bioorg. Med. Chem. Lett.* **1998**, *8*, 3665.
8. Michael, K.; Wang, H.; Tor, Y. *Bioorg. Med. Chem.* **1999**, *7*, 1361.
9. Cho, J.; Rando, R. R. *Biochemistry* **1999**, *38*, 8548.
10. Lacourciere, K. A.; Stivers, J. T.; Marino, J. P. *Biochemistry* **2000**, *39*, 5630.
11. Tok, J. B.-H.; Dunn, L. J.; Des Jean, R. C. *Bioorg. Med. Chem. Lett.* **2001**, *11*, 1127.
12. Hendrix, M.; Priestly, E. S.; Joyce, G. F.; Wong, C.-H. *J. Am. Chem. Soc.* **1997**, *119*, 3641.
13. Kirk, S. R.; Luedtke, N. W.; Tor, Y. *J. Am. Chem. Soc.* **2000**, *122*, 980.
14. Litovchick, A.; Evdokimov, A. G.; Lapidot, A. *Biochemistry* **2000**, *39*, 2838.
15. Faber, C.; Sticht, H.; Schweimer, K.; Rösch, P. *J. Biol. Chem.* **2000**, *275*, 20660.
16. Mei, H.-Y.; Cui, M.; Heldsinger, A.; Lemrow, S. M.; Loo, J. A.; Sannes-Lowery, K. A.; Sharmeen, L.; Czarnik, A. W. *Biochemistry* **1998**, *37*, 14204.
17. Dassonneville, L.; Hamy, F.; Colson, P.; Houssier, C.; Bailly, C. *Nucleic Acids Res.* **1997**, *25*, 4487.
18. Vicens, Q.; Westhof, E. *Structure* **2001**, *9*, 647.
19. Jiang, L.; Majumdar, A.; Hu, W.; Jaishree, T. J.; Xu, W.; Patel, D. J. *Structure* **1999**, *7*, 817.
20. Varani, L.; Spillantini, M. G.; Goedert, M.; Varani, G. *Nucleic Acids Res.* **2000**, *28*, 710.
21. Recht, M. I.; Douthwaite, S.; Dahlquist, K. D.; Puglisi, J. D. *J. Mol. Biol.* **1999**, *286*, 33.
22. McPike, M. P.; Goodisman, J.; Dabrowiak, J. C. *Methods Enzymol.* **2001**, *340*, 431.
23. McPike, M. P.; Goodisman, J.; Dabrowiak, J. C. *Bioorg. Med. Chem.* **2002**, *10*, 3663.
24. McPike, M. P.; Sullivan, J. M.; Goodisman, J.; Dabrowiak, J. C. *Nucleic Acids Res.* **2002**, *30*, 2825.
25. Sullivan, J. M.; Goodisman, J.; Dabrowiak, J. C. *Bioorg. Med. Chem. Lett.* **2002**, *12*, 615.
26. Coffin, J. M.; Hughes, S. H.; Varmus, H. E. *In Retroviruses*; Cold Spring Harbor Laboratory Press: Cold Spring Harbor, 1997.
27. Johnson, W. C., Jr. *Methods Biochem. Anal.* **1985**, *31*, 61.
28. Ennifar, E.; Pillart, J. C.; Marquet, R.; Ehresmann, B.; Ehresmann, C.; Dumas, P.; Walter, P. *J. Biol. Chem.* **2003**, *278*, 2723.
29. Lynch, S. R.; Gonzalez, R. L.; Puglisi, J. D. *Structure (Camb)* **2003**, *11*, 43.
30. Simonsen, K. B.; Ayida, B. K.; Vourloumis, D.; Takahashi, M.; Winters, G. C.; Barluenga, S.; Qamar, S.; Shandrick, S.; Zhao, Q.; Hermann, T. *Chembiochem.* **2002**, *3*, 1223.
31. Sucheck, S. J.; Wong, C.-H. *Curr. Opin. Chem. Biol.* **2000**, *4*, 678.